Egypt. J. Chem. **Vol. 67**, No. 10 pp. 475 - 486 (2024)

Egyptian Journal of Chemistry

http://ejchem.journals.ekb.eg/

The comparison effects of quinoa stalks activated carbon on adsorption of cadmium and lead polluted soils

Hend M. Nour[a], Hassan A. Khater[b], Asmaa A. Salem[a,*] and Noha H. Abdelkader[b]

[a] *Regional Center for Food and Feed, Agricultural Research Center, Giza, Egypt*
[b] *Soils Science Department, Faculty of Agriculture, Cairo University, Egypt*

Abstract

The study was performed to investigate the effect of activated carbons (ACs) in dose 2% w/w produced from agricultural wastes as Quinoa stalks (Q-AC), rice straws (R-AC) and corn stalks (C-AC) on different soils (clay and sandy loam) polluted by heavy metals (HMs) 100 mg Kg^{-1} cadmium (Cd_{100}), 600 mg Kg^{-1} Lead (Pb_{600}) or mixture of both elements (Cd_{100}/ Pb_{600}). The physical and chemical properties of ACs were assessed accordingly. The total carbon % values were higher in Q-AC (49.82%) than R-AC and C-AC, respectively. The surface area (BET) of AC samples was ranged from 489.3 to 1084.1 m^2 g^{-1}. The total pores volume (V_{total}) was increased in Q-AC (1.23 m^2 g^{-1}). SEM images proved high porosity of the Q-AC compared to R-AC or C-AC. The Fourier Transform Infrared spectroscopy (FTIR) analysis indicated the most porous activated carbon efficiency for adsorbing as carbonyl (C=O), carboxyl (C-O) and hydroxyl (–OH) groups in Q-AC played an important role in the adsorption process. Furthermore, the adsorption isotherm was examined the maximum adsorption capacity for Cd, Pb or mixture. Results showed that the highest adsorption capacity (Q_m) of Q-AC followed by R-AC and C-AC, respectively for individual Cd, Pb or mixture. In conclusion, the most effective AC was Q-AC followed by R-AC then C-AC in maximum adsorption capacity for Cd, Pb or mixture to remediate polluted soils according to their physical and chemical characteristics. The lignocellulose-rich agro-industrial waste produced effective activated carbons depending upon the total carbon content, surface area, pore size and volume, surface functionalities that offer economical and easy availability way to remediate the heavy metals polluted soils.

Keywords: soils remediation, cadmium, lead, activated carbon, agricultural wastes.

1. Introduction

Heavy metals (HM) contamination in soil has become a major problem for many countries throughout the world. Lead (Pb) and cadmium (Cd) usually in higher concentrations may result in poor environmental quality by reducing crop productivity and groundwater toxicity causing serious threat to human and animal health. Therefore, contaminated soils restoration is a major priority for animal and food production. In addition, HM are non-biodegradable in nature and toxic, even at very low concentrations [1, 2]. Heavy metals occur naturally in Earth crust and natural processes which are released into soil by various human activities [3]. The availability reduction of HM is the key for remediation of contaminated soils. Different techniques reduce HM accumulation in soil as physical remediation to be more cost saving. Physical soil remediation used for cleaning up or control/reduce the environmental risks of soil contaminants. It has advantages of low cost, high remediation efficiency, wide source of raw materials, eco-friendliness and soil improvement. Adsorbents have porous surface, high pH values, and active surface functional groups [4, 5, 6]. Activated carbon has recently attracted the attention because of its significantly high adsorption capacity against heavy metals. The large surface area, suitable surface functional groups, and appropriate pore diameter make activated carbon a potential adsorbent [7]. Porous carbon materials which had large specific surface areas and high adsorption performance were prepared toward the industrial applications [8].

Utilization of agricultural wastes to produce valuable products to minimize serious public health risks from exposure to dangerous fumes that come from burning the agricultural wastes in open fields [9, 10]. Activated carbon (AC) can be derived from cellulose, hemicellulose, lignin and other components in lignocellulose materials [11]. World quinoa (*Chenopodium quinoa*) production is increasing due its

*Corresponding author e-mail: namesaaa2013@gmail.com; Asmaa A. Salem
EJCHEM use only: Received date 12 March 2024; revised date 10 June 2024; accepted date 25 June 2024
DOI: 10.21608/ejchem.2024.275802.9433

high nutritional value. As a consequence, large quantities of stalks accumulate as unused by-products. Stalks are a natural source of lignocellulosic biomass, which include lignin and a variety of polysaccharides such as cellulose which causing cheap and valuable source for producing the highly porous activated carbon materials [10, 12]. Rice straw low cost agriculture wastes consist of hemicellulose (35.7%), cellulose (32%), lignin (22.3%) and extractive materials. It was used to produce AC which exhibits excellent absorption performance due to its high surface area, porosity (large pore volume) and rich in active functional groups [11, 12].

The aim of our work is the evaluation of chemical and physical properties for Q-AC, R-AC and C-AC as different prepared activated carbons. Comparison study for the effect of Q-AC, R-AC and C-AC (2%, w/w) on remediation of different concentrations of heavy metals (Cd or / and Pb, individual or mixture) on polluted soils (clay and sandy loam) by confirming the maximum capacities adsorption isotherm for heavy metals.

2. MATERIALS AND METHODS

2.1. Materials

Cadmium chloride ($CdCl_2.H_2O \geq 99\%$ purity) and lead chloride ($PbCl_2 \geq 99\%$) were provided by Fluka, Tunisia. All the chemicals were used as received without purification and salts solution were prepared by deionized water.

2.2. Preparation of the activated carbons

Quinoa stalks (Q), rice straws (R) and corn stalks (C) samples were collected from the Agricultural Research center (Giza, Egypt). All samples were washed water, dried in an oven (Model UF110, Germany) at 105°C for 16 h [13]. Production of activated carbon via pyrolysis at 700°C for 45 min followed by steam activation of the samples at temperature 250°C for 60 min [14].

2.3. Chemical and physical Characterizations of ACs

Physical and chemical basic characteristics of Q-AC, R-AC and C-AC samples were assessed. The total carbon content was measured by CNHOS element analyzer (Elementor Vario EL III, Elementar Analysensysteme GmbH, Germany). Cation exchange capacity (CEC, $Cmol_c kg^{-1}$) was detected according to Hissink's method [15]. pH and electrical conductivity (EC, dSm^{-1}) were examined by soaking ACs in distilled water, boiling for 5 min. then cooling which EC values were measured in the suspension and supernatant [16]. Percent of moisture content was estimated by drying samples at 105°C [17]. Ash content (%) of samples was determined by muffle furnace at 440°C which the substance remaining after ignition is the ash [17]. In addition, Total surface area (BET) and porosity of the Q-AC, R-AC and C-AC samples were evaluated using N_2 adsorption analysis (Micromeritics ASAP 2010) at 77 K. The samples were degassed prior to be analyzed under vacuum at 110°C for 10 h. BET analysis were used to measure the surface area, pore volume, and pore size using the Micromeritics ASAP 2020. Scanning electron microscopy (SEM) of FEI model Quanta 400 was used to observe surface morphology of the samples. (Bruker, Alpha). Chemical functional groups of the samples surface were analyzed using Fourier-transform infrared spectroscopy (FTIR) was measured between 400 and 4000 cm^{-1} by using Bruker Vector 22 spectrometer (Vector 22, Bruker, USA) using a FTIR Spectrometer instrument.

2.4. Heavy metals Adsorption isotherms

Cd and Pb adsorption mechanism was ascertained by the Langmuir adsorption isotherms. The experiments were conducted by utilizing the batch technique, with preliminary concentrations of solutions varying from 1-200 mg/L. One gram of soil was shaken with 10 ml 0.01M $CaCl_2$ containing Cd or Pb concentrations of l, 5, 10, 50, 100 and 200 ppm for 24 hours at 25°C.After shaking, soil solution was filtered through Whatman No.42 filter paper. The concentration of heavy metals (Cd, Pb) of adsorption isotherm supernatants solution were determined according [18], using atomic absorption spectrophotometer (Perkin-Elmer model 1100B, USA). The data were fitted to the Freundlich model of isotherm:

A. Langmuir Model

$Ce/(x/m) = 1/k_d + Ce/Q_m$

Where,

x/m = Amount of ion adsorbed per unit weight of soil ($mg\ kg^{-1}$)

Ce = Equilibrium concentration in soil solution ($mg\ l^{-1}$)

k_d = a constant related to bonding energy of ion to the soil.

Q_m = the maximum adsorption capacity of soil.

B. Freundlich Equation

$\log x/m = \log K_d + 1/n \log Ce$

Where, x/m = Amount of ion adsorbed per unit weight of soil ($mg\ kg^{-1}$)

Ce = Equilibrium concentration in soil solution ($mg\ L^{-1}$)

K_F = a function of energy of adsorption and temperature and is a measure of partitioning coefficient 1/n determines intensity of adsorption.

The adsorption isotherm can be determined once obtaining the equilibrium time of adsorption. These experiments were carried out until the adsorptions obtained equilibrium. The relation between the quantities of adsorbed heavy metals by such soil (q) the concentrations of solutions having heavy metal at equilibrium Ce is known as an adsorption isotherm.

3. Statistical analysis

A randomized complete block design with three factors was used for analysis all data with three replications. The treatment means were compared by least significant difference (L.S.D.) test as given by [19]. Statistical analysis was carried out by special statistical program "Assistat" [20].

4. Results & Discussion

4.1. Chemical and physical properties of activated carbon samples (Q-AC, R-AC and C-AC)

The results in Table (1) showed the physical and chemical properties of activated carbons produced from quinoa stalks (Q-AC), corn stalks (C-AC) and rice straw (R-AC). The results indicated that the percent of total carbon in Q-AC (49.82%) were higher than R-AC

Table 1. Some physical and chemical properties of activated carbons

Activated carbons	Total carbon (TC) %	Silica (SiO_2) (%)	CEC ($Cmol_c kg^{-1}$)	EC (dSm^{-1})	pH	ASH (%)	Moisture (%)	Surface area (BET) (m^2/g)	V_{total} (m^2/g)	Pore size (nm)
Q-AC	49.82	3.94	42.53	28.30	8.60	15.20	12.00	1084.12	1.23	12.00
R-AC	45.15	11.35	36.51	17.60	8.30	13.25	11.60	706.56	0.76	18.00
C-AC	42.36	3.70	24.10	7.30	8.00	7.90	9.10	489.31	0.59	26.00

Q-AC: Quinoa stalks, R-AC: rice straws, C-AC: corn stalks, activated carbons, CEC: Cation exchange capacity, EC: electrical conductivity, V_{total}: total pore volume

High total carbon sources of ACs were cellulose, hemicellulose, lignin, and soluble sugar. ACs had some unsaturated carbon bonds, carboxyl groups, hydroxyl groups, and other groups that were easily combined with heavy metal ions (positively charged) through hydrogen bonds or ion exchange [21]. In addition, Cellulose, hemicellulose, and lignin are main components of quinoa husk (QH). Carbon content of raw materials is a good precursor for activated carbon sources. Elevation of ash% may related to increasing in mineral contents which contributed to their relatively high pHs [22]. Moreover, the surface area of porous carbon quinoa husk (PC–QH) was carbonized at 650°C / 90 min (pH 7) was 1713 (m^2/g) [12]. The BET and the total volume pores are directly proportional with increasing the number of pores [22, 23]. Highest porosity is related with BET, pore size and adsorptive capacity [24].

(45.15%) and C-AC (42.36%) respectively, whereas the percent of silicate in R-AC (11.35%) was higher than Q-AC and C-AC respectively. The value of Cation exchange capacity (CEC) in Q-AC (42.35 $Cmol_c kg^{-1}$) was greater than R-AC and C-AC, likewise EC, Ash, PH and Moisture in the ACs samples. The porosity results showed an enhancement in Q-AC were total pore volume (1.23 (m^2/g) compared to R-AC and C-AC respectively, then the pore size in all ACs were ranged from 12 to 26 nm. Surface area (the Brunauer–Emmett–Teller theory, BET) recorded 1084.1 m^2/g in Q-AC, 706.5 in R-AC and the lowest value in C-AC which was 489.3 m^2/g.

4.2. The SEM activated carbon structure of quinoa stalks (Q-AC), rice straw (R-AC) and corn stalks (C-AC)

The activated carbon surface structures of Q- AC, R-AC and C-AC were scanned by SEM and the results were shown in (Fig. 1-3).

Differences in surface properties were clearly observed in SEM images among Q-AC, R-AC and C-AC, with all showing fibrous channels.

The SEM image of Q – AC was observed (Fig.1) which showed that the structure consisted of a highly complex network of pores. The SEM of activated carbon particles have a rough surface with plenty pores and cracks on their surface.

The pore size of Q-AC was (12 μm) while the pore sizes of R-AC and C-AC were (16, 28 μm), respectively. The highest surface area was 1084.1 m^2/g in Q-AC compared to R-AC which was 706.5 and the lowest surface area of C-AC was 489.3 m^2/g. The dark and light zones expressed to carbon structure contained porous morphology and small particles on its surface and several metal oxides on the carbon sheets [21, 25]. Scanning electron microscope imaging indicated that charges on the surface of ACs which were located in small and large pore layers [26]. Physical activation caused relatively large sized pores with no uniformly on the surface of ACs due to the loss of primary bonds in the raw materials and the formation of new bonds [27]. Activation produced

4.3. The FTIR spectra of quinoa stalks (Q-AC), corn stalks (C-AC) and rice straw(R-AC)

The FTIR spectral analysis detected the presence of organic substances, bonds type, identifying characteristic functional groups and determining the reactivity of Q-AC, R-AC and C-AC to observe the porous activated carbon efficiency for adsorbing. Infrared absorption is in the range of k = 400 cm^{-1} to k = 4000 cm^{-1} was measured for Q-AC, R-AC and C-AC [Fig. 4 to 6]. The FTIR spectrum of ACs were significant differences between their characteristic peaks at different wave numbers which functional groups accountable for the adsorption characteristics. The data of FTIR on Q-AC (Fig. 4) represented that peak at position 3464.15 cm^{-1} was (O – H) hydroxyl

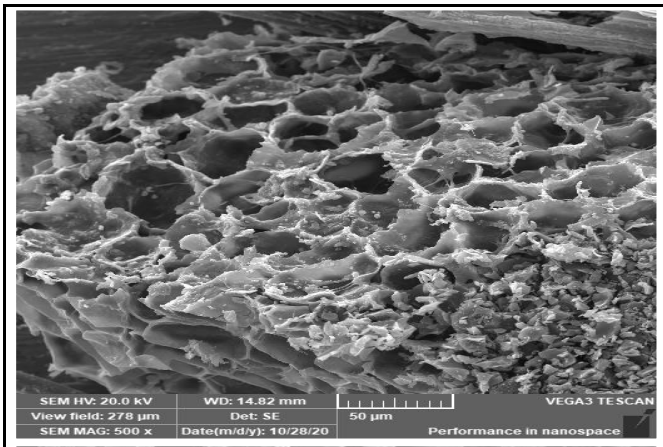

Fig.1. The SEM images of Quinoa stalks activated carbon (Q-AC)

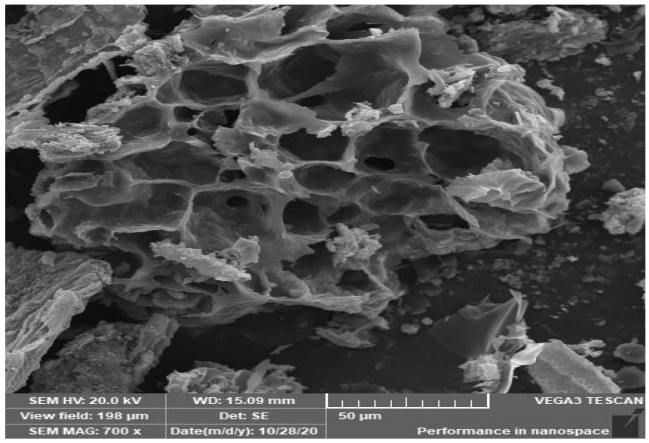

Fig. 2. The SEM images of rice straw activate carbon (R-AC)

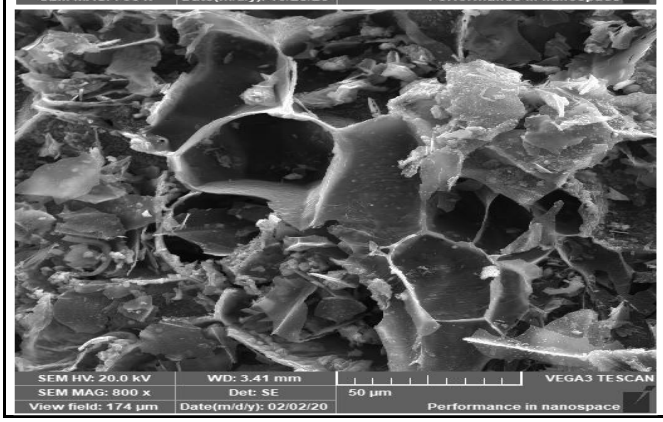

Fig. 3. The SEM images of corn stalks activated carbon (C-AC)

Fig 1-3. The SEM analysis of all activated carbons

group (alcohol, phenol). Whereas, peaks at positions 2885.51 cm−1 and 1396.46.64 cm^{-1} showed (C-H, alkanes). While, peaks at position 1635.64 (cm^{-1}) for (C=O) bond and 1103.28(cm−1) (C-O) bond represented the carboxylic groups (−COOH). Fig. 5 showed FTIR on R-AC that position peak at 3456.44 cm^{-1} was (O-H alcohol, phenol), 1635.64 cm^{-1} (C=O, carboxylic acid) and 1388.75 cm^{-1} (C-H, alkanes), respectively. FTIR of C-AC represented at Fig. 6, positions 3502.73 and 3464.15 cm^{-1} for (O-H alcohol, phenol), 1388.75 cm^{-1} for (C-H, alkanes) respectively. Similar tendencies have been reported by [27, 32, 33]. The active functional groups charge on surface of AC such as hydroxyl, carboxyl, and carbonyl are responsible for the metals adsorption by forming metal hydroxide, carbonate, and specific metal ligand complexation [25]. Functional groups of activated carbons caused electrostatic attraction between surface oxygen-containing and the metal ions [28]. The FTIR spectrum detected the characteristic functional groups found in the carbonaceous materials which confirmed the successful activation process [22]. It was observed that the presence of hydroxyl and carboxyl groups were responsible for adsorption process. The bands observed at 3391 cm^{-1} for hydroxyl groups (O-H) while, at 1622 cm^{-1} is attributed to C=O and C-O stretching of carboxylic acid at 1398 cm^{-1} [22].

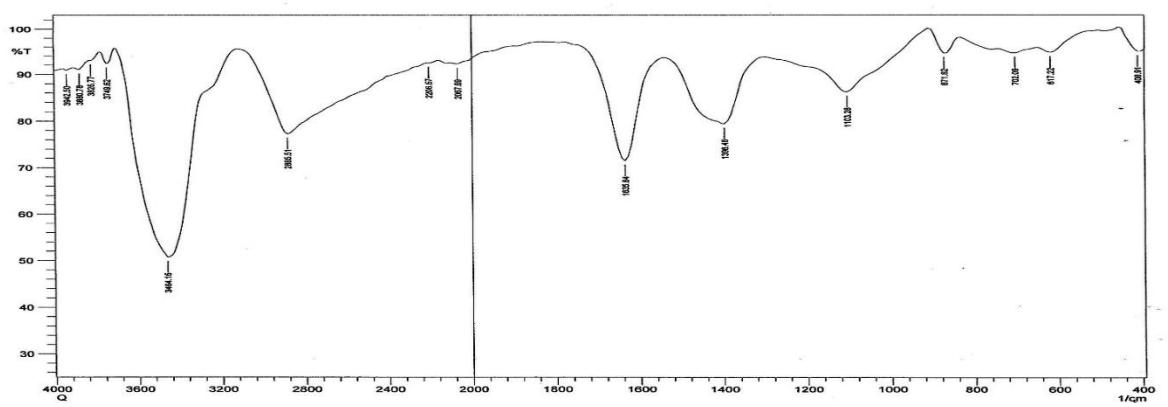

Fig. 4. The FTIR spectra of quinoa stalks Q-AC

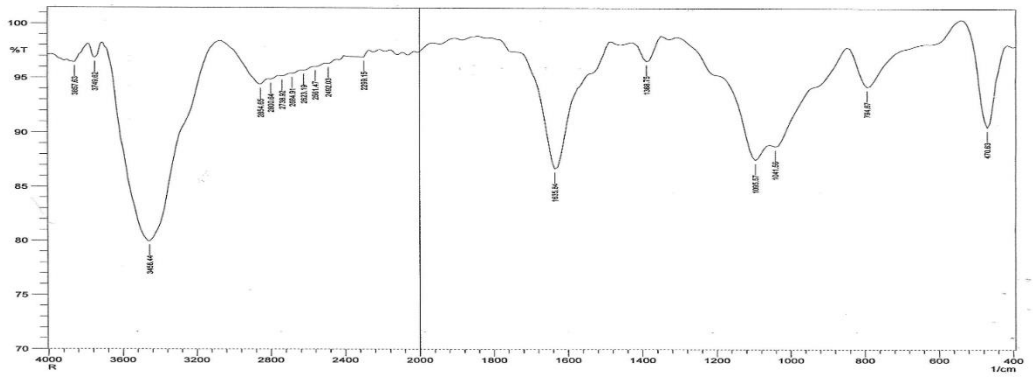

Fig. 5. The FTIR spectra of rice straw R-AC

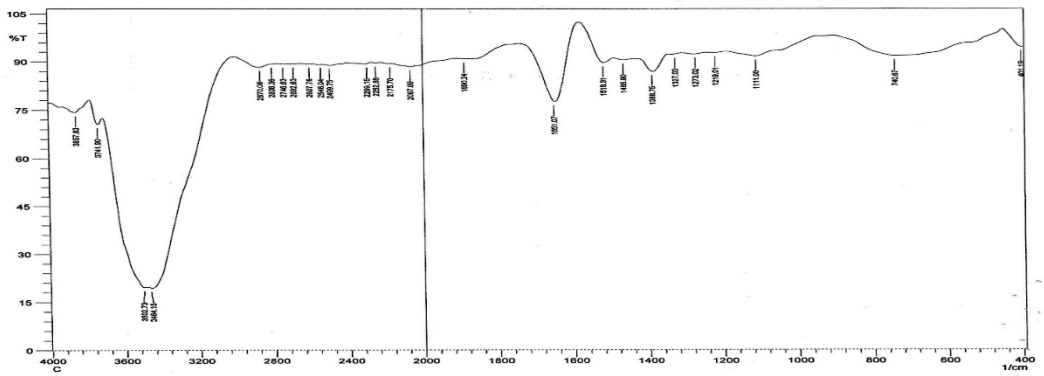

Fig.6. The FTIR spectra of corn stalks C-AC

It was observed the structure of cellulose ($C_6H_{10}O_2$) as primary material to prepare AC the bonds OH were k=3421 cm^{-1} and confirmed that carbon is not lost during the carbonization process [27]. The C=O of the carbonyl group was showed at the peak 1650 cm^{-1} but the C-O stretching vibrations adjacent to the quinone and hydroxy groups of AC on the peak at 1100 cm^{-1} was related to the phenolic hydroxyl and carboxylic group [34]. IR spectra of raw rice straw showed O–H extended from holocellulose (cellulose and hemicellulose) at 3300 cm^{-1} but at 3743 cm^{-1} for O–H for the prepared carbonized rice straw due to heating, carbonization, and activation processes which gave a good surface with numerous functional groups for the metal adsorption.

The characteristic peak of acetyl group C=O at 1736 cm^{-1} is owing to hemicellulose/lignin while, the absorption of C–O–C band was at 1035 cm^{-1} [33]. The decomposition of glycosyl units followed by its transformation to char during corn stalk activation. The FTIR spectra broad peak at 3350 cm^{-1} caused by the OH group [35]. Formation of O–H, C–O groups on activated carbon surface resulted in increasing its porosity and specific surface areas [36]. The sharp bands near 455 cm^{-1} define the Si–OH stretches. The band at 1095.50 cm^{-1} is Si-O-Si and those at 1442.75 and 1654.92 are C=O groups. The sharp peaks at 2870.08, 3248.13 and 3614.60 are the O-H stretch [37]. This is also advantageous, since activated carbons of relatively higher specific surface area may be obtained, once the desilicated rice husks are activated [38].

4.4. Adsorption isotherm:

The experimental data of the Langmuir adsorption isotherms curves were fitted to the linear forms of Cd 100 mg Kg^{-1}, Pb 600 mg Kg^{-1} and mixture Cd 100/ Pb 600. Initial concentrations of Cd and Pb were l, 5, 10, 50, 100 and 200 ppm to study the linear form model of adsorption in clay and sandy loam soils after one day (1D) and two months (2M) with Q-AC, R-AC and C-AC (2%) comparing to the control. The adsorbed amounts of Cd or Pb were calculated as the difference between their initial and final concentrations in the solutions. The Results showed in Figures 7 to14 that the amount of individual adsorbed (x/m; mg Kg^{-1}) Cd 100 in clay and sandy loam soils (mg kg^{-1}) for 1D increased after 2 M but The adsorbed Cd in mixture Cd 100/ Pb 600 was lower compared to the individual Cd 100. The results by adding ACs indicated that the highest adsorbed curves were in Q-AC followed by R-AC then C-AC, respectively for either individual Cd or the mixture. Generally, the highest adsorbed curves were recorded in the clay soil than the sandy loam soil. The obtained adsorption isotherm curves were presented in Figures (7 to 22) these all the investigated metals (Cd and Pb) were increased with increasing the equilibrium concentration which figures were showed the typical metals adsorption isotherms by different soils. These adsorption curves were fitted to the linear forms of Langmuir models.

Results showed in Figures 15 to 22 that the amounts of individual adsorbed Pb 600 (x/m; mg/Kg) in clay and sandy loam soils (mg kg^{-1}) for 1D which increased after 2 M but The adsorbed Pb in mixture Cd 100/ Pb 600 was lower compared to the individual Pb 600. The results by adding ACs indicated that the highest adsorbed curves were in Q-AC followed by R-AC then C-AC, respectively for either individual Pb or the mixture. The adsorbed Pb amounts in the sandy loam soil were lower than in the clay soil.

In the equilibrium state, it is important to study the adsorption isotherm. Thus, the utilized contact time was 2 months for evaluation. In order to explain the isotherm, models of Langmuir and Freundlich adsorption isotherms have been adopted. From the data summarized in Tables 2 and 3 which were established the Langmuir as a model that best describes the adsorption of heavy metals (Cd and Pb) the parameters of the Freundlich and Langmuir isotherms,

where x/m (mg k^{-1}) is the quantity of adsorbed metal and C_e (mg l^{-1}) is the concentration of equilibrium. The maximum adsorption capacity (Q_m) and partitioning coefficients (binding energy) (K_F) were obtained from Langmuir model in Table (2and 3). The adsorption isotherm showed that the capacity of Q-AC to adsorb and remove nutrients cations "Cd^{+2}"and " Pb^{+2} "from soils was higher than R-AC and C-AC, respectively particularly at the higher equilibrium concentration. These results indicated that addition even small quantities of Q-AC to soil will increase capacity of soil to adsorb the heavy metals. Generally, the quantities of Pb adsorbed on ACs are much lower than their corresponds of Cd which indicated the high capacity of these materials to adsorb Cd rather than Pb. Also, it could be attributed to the property of Cd element which could be removed from solution by electrostatic attraction to negatively charged sites, hence exist as exchangeable cations, which is not a character for Pb. Adsorption equations, the validity of Cd and Pb adsorption data to linear forms of both Freundlich and Langmuir models were examined. Also, the amounts of both Q_m and K_F have been calculated using Langmuir models. Cadmium and lead adsorption data were found to fit both Freundlich and Langmuir equations. High correlation coefficients (R^2 ranging from 0.891-0.981 and 0.879-0.977) were obtained for Langmuir isotherms of Cd and Pb, respectively. Their corresponding values of Freundlich (R^2) are ranging from 0.74 - 0.99 and 0.78-0.99 for Cd and Pb, respectively.

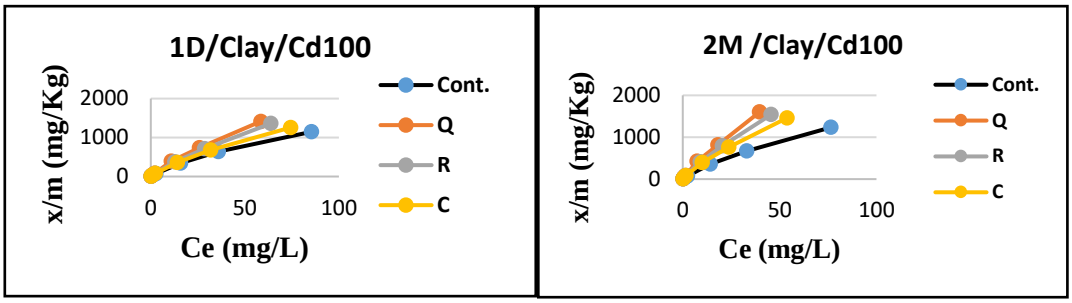

Fig.7 and 8. Adsorption isotherm curves of Cd100 by Q-AC, R-AC and C-AC in clay soil for 1D and 2M

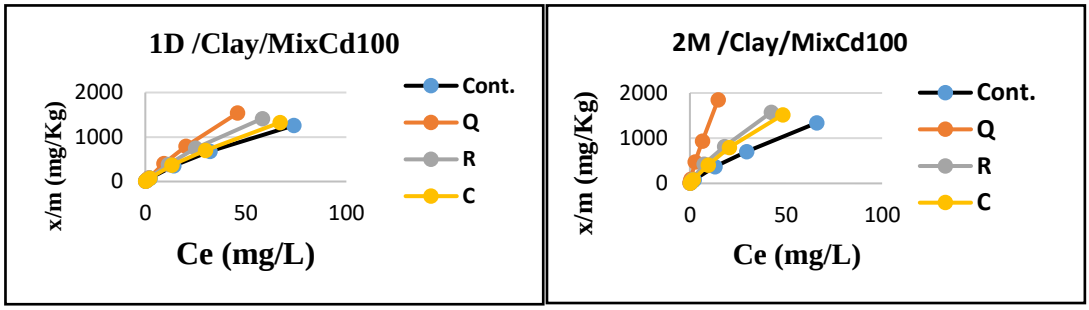

Fig. 9 and 10. Adsorption isotherm curves of mix. Cd100 by Q-AC, R-AC and C-AC in clay soil for 1D and 2M

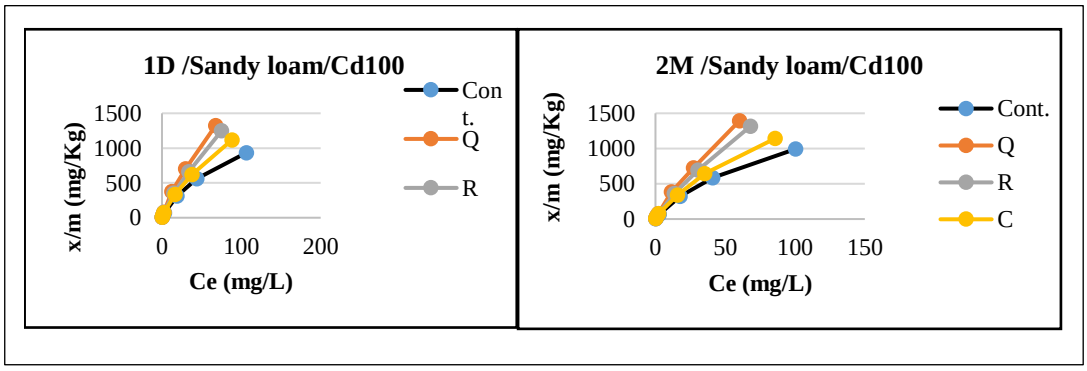

Fig. 11 and. 12. Adsorption isotherm curves of Cd100 by Q-AC, R-AC and C-AC in sandy loam soil for 1D and 2M

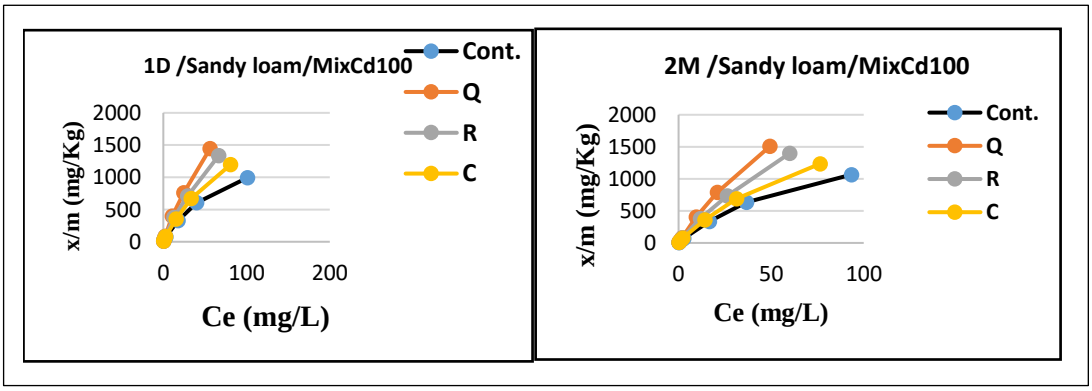

Fig. 13 and 14. Adsorption isotherm curves of mix. Cd100 by Q-AC, R-AC and C-AC in sandy loam soil for 1D and 2M.

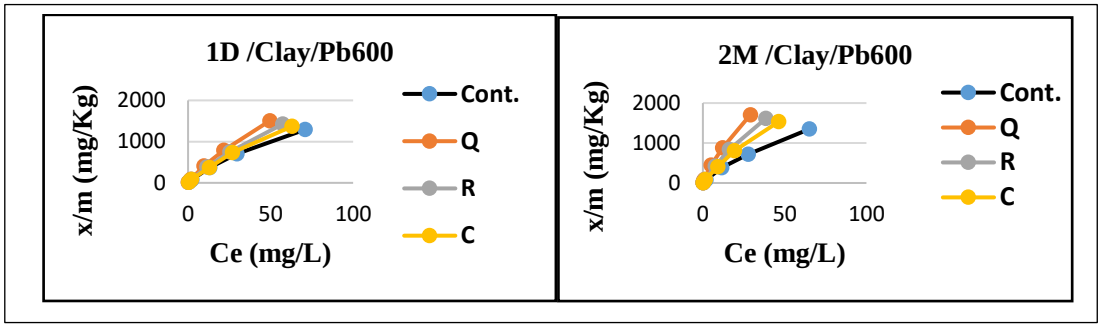

Fig. 15 and 16 Adsorption isotherm curves of Pb600 by Q-AC, R-AC and C-AC in clay soil for 1D and 2M

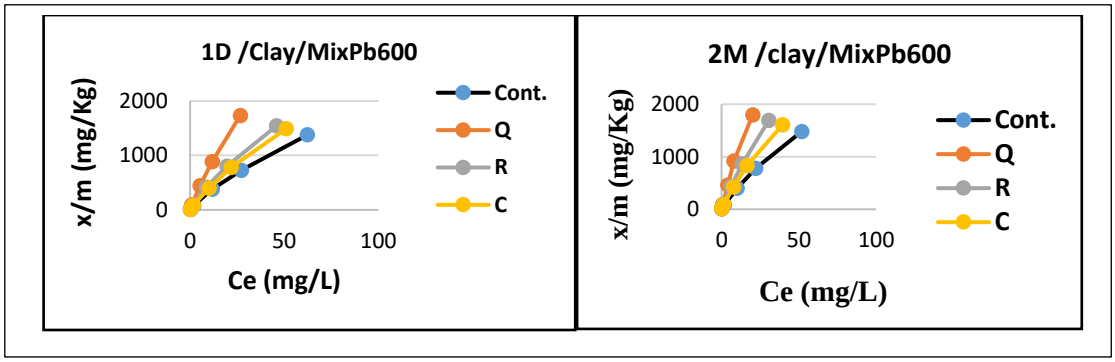

Fig. 17 and 18 Adsorption isotherm curves of mix. Pb 600 by Q-AC, R-AC and C-AC in clay soil for 1D and 2M

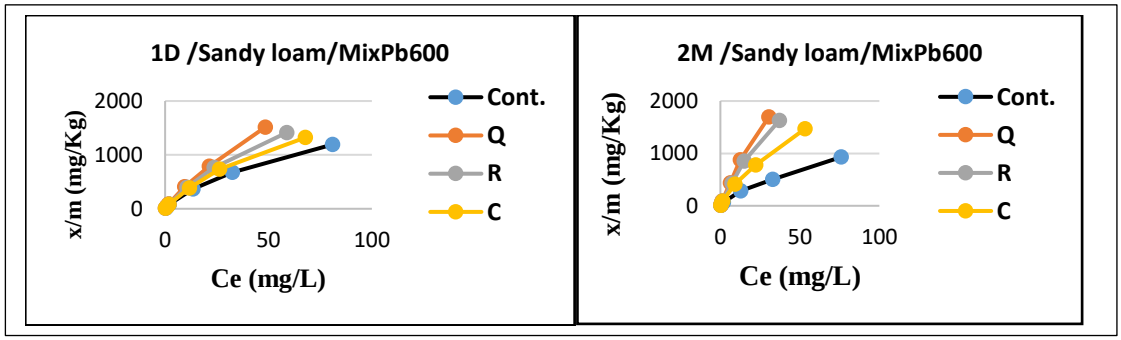

Fig. 19 and 20. Adsorption isotherm curves of Pb600 by Q-AC, R-AC and C-AC in sandy loam soil for 1D and 2M

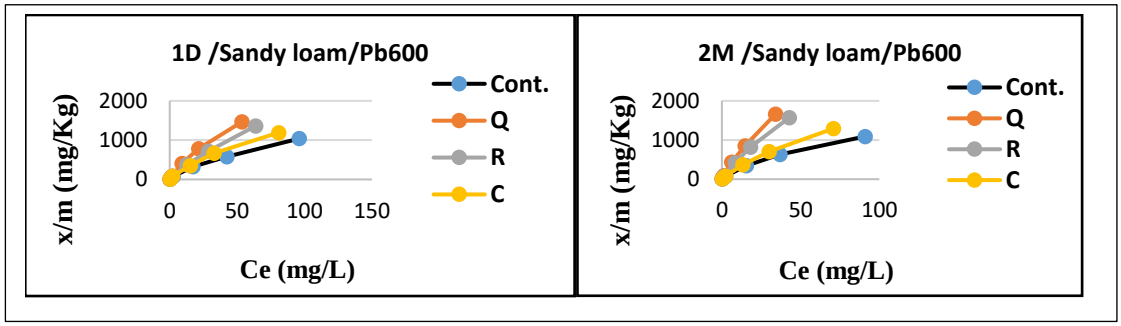

Fig. 21and 22. Adsorption isotherm curves of mix. Pb 600 by Q-AC, R-AC and C-AC in sandy loam soil for 1D and 2M

Table 2. Maximum adsorption capacity (Qm) and binding affinity (KF) of Q-AC, R-ACs and C-AC for Cd in clay and sandy loam soils for 1D and 2M.

Soil	ACs (2%)	Time	Q_m (mg g^{-1})		K_F(L g^{-1})	
			Cd 100	Cd 100 mix.	Cd 100	Cd 100 mix.
Clay	Control	1D	441.17	370.26	0.0116	0.0111
		2M	535.71	498.50	0.0137	0.0131
	Q-AC	1D	576.90	554.56	0.0186	0.0178
		2M	681.68	652.17	0.0219	0.0209
	R-AC	1D	553.56	483.87	0.0156	0.0149
		2M	625.01	601.65	0.0183	0.0175
	C-AC	1D	504.10	441.18	0.0135	0.0129
		2M	576.92	552.56	0.0159	0.0152
Sandy loam	Control	1D	405.41	340.91	0.0106	0.0101
		2M	483.87	454.55	0.0125	0.0119
	Q-AC	1D	535.71	468.75	0.0170	0.0162
		2M	624.99	597.00	0.0201	0.0190
	R-AC	1D	416.70	416.70	0.0143	0.0135
		2M	576.92	557.56	0.0168	0.0159
	C-AC	1D	384.62	375.00	0.0124	0.0119
		2M	535.71	517.23	0.0146	0.0140

ACs: Activated carbons, Quinoa stalks (Q-AC), rice straws (R-AC) and corn stalks (C-AC) activated carbons in concentrations 2%., 1D: for one day, 2M: for two months, Qm: Maximum adsorption capacity, KF: affinity, Cd 100: Cd in concentration 100 mg. Kg^{-1}, Cd 100 mix.: Cd in mixture of Cd/Pb in concentration 100 mg. Kg^{-1}.

Table 3. Maximum adsorption capacity (Qm) and binding affinity (KF) of Q-AC, R-AC and C-ACs for Pb in clay and sandy loam soils for 1D and 2M.

Soil	ACs (2%)	Time	Q_m (mg g^{-1})		K_F (L g^{-1})	
			Pb600	Pb600 mix.	Pb600	Pb600 mix.
Clay	Control	1D	882.35	776.20	0.0185	0.0176
		2M	1094.88	993.38	0.0218	0.0207
	Q-AC	1D	1162.79	1020.41	0.0326	0.0310
		2M	1363.64	1304.35	0.0383	0.0364
	R-AC	1D	1041.60	949.37	0.0272	0.0259
		2M	1327.43	1209.68	0.0321	0.0304
	C-AC	1D	943.35	857.14	0.0229	0.0218
		2M	1209.68	1094.89	0.0270	0.0256
Sandy loam	Control	1D	778.20	721.15	0.0168	0.0149
		2M	993.38	949.37	0.0198	0.0175
	Q-AC	1D	1020.41	974.23	0.0298	0.0285
		2M	1304.34	1239.67	0.0351	0.0335
	R-AC	1D	949.37	903.61	0.0248	0.0236
		2M	1209.68	1153.85	0.0292	0.0277
	C-AC	1D	857.14	824.18	0.0208	0.0200
		2M	1094.88	1048.95	0.0245	0.0236

ACs: Activated carbons, Quinoa stalks (Q-AC), rice straws (R-AC) and corn stalks (C-AC) activated carbons in concentrations 2%, 1D: for one day, 2M: for two months, Qm: Maximum adsorption capacity, KF: adsorption affinity (binding energy), Pb 600: Pb in concentration 600 mg. Kg^{-1}, Pb600 mix.:Pb in mixture of Pb / Cd in concentration 600 mg. Kg^{-1}.

The results indicate the Q_m of the tested ACs (Q-AC, R-AC and C-AC) to adsorb Cd ranged from 441.18 - 681.68 mg g^{-1} Cd in clay soil and 375 - 624.99 mg g^{-1} Cd in sandy loam soil, respectively. The adsorption affinity (binding energy) (K_F) between ACs for Cd ranged from 0.0129 to 0.0219 in the clay soil and 0.0119 to 0.0190 in the sandy loam soil, respectively. The highest value of K_F (0.0219) was recorded for binding affinity Q-AC to Cd, whereas the lowest one (0.0119) in C-AC belongs to Cd. On the other hand, Q_m to adsorb Pb ranged from 1094.89 - 1363.64 mg g^{-1} Pb in the clay soil and ranged 824.18 - 1304.34 mg g^{-1} Pb in the sandy loam soil, respectively. K_F of tested ACs for Pb ranged from 0.0218 to 0.0383 in the clay soil and 0.0200 to 0.0351 in the sandy loam soil respectively. The highest value of K_F (0.0383) was showed in Q-AC, whereas the lowest one (0.0200) for C-AC. One of the most important characteristics of the soil is the quantity of the metal that it can accumulate. The amount of metal adsorbed was calculated from the difference between the added and the equilibrium metal concentrations to establish the Langmuir was the model in adsorption of ions with $R^2 > 0.90$ in all cases [35]. Clay soils

indicated the dominance of inner-sphere type surface complexing mechanisms, or to significant adsorption processes mediated by van der Waals interactions. The sequence of affinity of the tested metals in the investigated soils was found to be the following: Pb > Cd. The adsorption process occurs as a mono layer [37]. High adsorption capacity of Cd and Pb could be attributed to the high number of functional groups exis on ACs, these groups particularly those contain oxygen, e.g —OH and C=O through ligand exchange mechanism ions. Anion can only be adsorbed through cation exchange on the sites carrying negative charge which is dependent on the value of CEC, which is limited comparing with the large number of functional groups. Ions are adsorbed on the sites of low binding affinity so they are easily to be desorbed [32]. The main physical adsorption mechanism was controlled by Van der Waals forces and electrical attraction because pores had active adsorption sites with high surface area. Chemical bonds were formed between functional groups of ACs (C=O, N-H, and O-H) and the metals forming complexation [39]. Heterogeneous surface of the bio-adsorbents prepared from corn stalks showed different activation energies for reactions because their cell walls primarily consist of cellulose, and many hydroxyl groups, such as tannins or other phenolic compounds [35].The high Q_m values observed for dye adsorption (positively charged) on the carbon surface (cellulosic materials, negatively charged) in mono- and multilayers. The adsorbent surface is positively charged, there will be a stronger electrostatic interaction between them [22]. The highest ability Qm, the order of affinity of Lead and Cadmium for the investigated soil occurred at Pb > Cd, and the maximum capacities of adsorption of competition of two cations are decreased for the same effective sites. In addition, it focuses on the behaviors of the adsorption of lead and cadmium in several environmental soils. The quantity of heavy metal was overmuch as compared to the sites of adsorption at higher concentrations [40]. Moreover, Combined system for the adsorption capacity was decreased which process occurs as a mono layer. The Langmuir model gives the best fit for the experimental data for single, binary and ternary component adsorption system for lead, copper and cadmium ions recognized by the highest values of (R^2). This indicates that the adsorption The adsorption capacity Q_m for Pb is greater than Cd in single system, Q_m of Pb^{2+} was 76.104 mg/g > Cd^{+2} (30.254 mg/g). This behavior may be attributed to several reasons from which the hydrated ionic radius. The ions with hydrated radius smaller than the pore size are able to move easily within the pores [37]. Heavy-metal (Cd) fixation by AC mostly depend on AC surface pore size, oxygen-containing functional groups, the pyrolysis temperature used in AC preparation, and soil characteristics [41], found that the adsorption capacity of Q-AC increased by increasing pH [12]. It was suggested that OH^- provide extra adsorption sites leading to greater adsorption capacity of Cd ions forming Cd phosphate and carbonate minerals through complexation. High pH > 4.5, the adsorption increased rapidly to the maximum value. In addition, these differing adsorption capacities followed by different equilibrium pH values were probably related to the presence of ash and alkaline substances that originated from pyrolysis, which might be desorbed from the rice straw AC surface. The increased surface area, physical changes in porous structure and surface functionality (H^+) of COO^- and O^-groups might be the main reasons to increased heavy metal adsorption by AC [42]. Our findings were in compliance with, [37], who concluded that Pb adsorbed more strongly than Cd, respectively. The results showed hydroxyl and carbonyl groups shifted to higher transmission (peaks of adsorption) of these ions.

5. Conclusions

The prospective uses of agricultural wastes for industry as raw materials to reduce the environmental pollution and save economical adsorbents production cost. It was recommended to use of the Quinoa stalks (Quinoa, a recent wheat substitutes) which considered as field wastes as a precursor for synthesis of an effective low-cost activated carbon using a simple method for heavy metals adsorption from contaminated soils comparing to activated carbon produced from traditional crop wastes as rice straws and corn stalks. The addition of the Quinoa stalks activated carbon as heavy metal adsorbent in both clay and sandy loam soils improve the heavy metal as lead and cadmium adsorption.

6. Conflicts of interest

"There are no conflicts to declare".

7. Fund

The authors have no fund.

8. References

[1] C. M. Raffa, F. Chiampo, and S. Shanthakumar, "Remediation of Metal/Metalloid-Polluted Soils: A Short Review," Applied sciences, vol. 11, p. 4134, 2021.

[2] Z. Zhang, T. Wang, H. Zhang, Y. Liu, and B. Xing, "Adsorption of Pb(II) and Cd(II) by

magnetic activated carbon and its mechanism," Science of the Total Environment, vol. 757, p. 143910, 2021.

[3] S. Khalid, M. Shahid, N. K. Niazi, B. Murtaza, I. Bibi, and C. Dumat, " A comparison of technologies for remediation of heavy metal contaminated soils," Journal of Geochemical Exploration, vol. 182 , pp. 247-268, 2017.

[4] Y. Hamid, L. Tang, X. Wang, B. Hussain, M. Yaseen, M. Z. Aziz, and X. Yang, "Immobilization of cadmium and lead in contaminated paddy feld using inorganic and organic additives," Scientific Reports, vol. 8, p. 17839, 2018.

[5] Y. Wang, H. S. Wang, C. S. Tang, K. Gu, and B. Shi, "Remediation of heavy metal-contaminated soils by biochar: a review," Environmental Geotechnics, vol. 9, Issue 3, pp. 135-148, 2019.

[6] E.A. Abdel-Galil, H.E. Rizk, and W.M. El-kenany, "Low Cost Natural Adsorbent for Removal of Pb (II) Ions from Waste Solutions," Arab J. Nucl. Sci. Appl., Vol. 51, no. 4, pp. 19-30, 2018.

[7] A. Othmani, J. John, H. Rajendran, A. Mansouri, M. Sillanpa, and P. V. Chellam, "Biochar and activated carbon derivatives of lignocellulosic fibers towards adsorptive removal of pollutants from aqueous systems: Critical study and future insight," Separation and Purification Technology, vol. 274, p. 119062, 2021.

[8] D. Liang, X. Tian, Y. Zhang, G. Zhu, Q. Gao, J. Liu, and X. Yu, "A Weed-Derived Hierarchical Porous Carbon with a Large Specific Surface Area for Efficient Dye and Antibiotic Removal," International Journal Molecular Sciences, vol. 23, p. 6146, 2022.

[9] M. El Zayat, and E. Smith, "Removal of Heavy Metals by Using Activated Carbon Produced from Cotton Stalks ,"Canadian Journal on Environmental,Construction and Civil Engineering, Vol.1, No. 4, pp. 71-77, 2010

[10] A. G. Ramireza, D. M. S. Veizagab, C. Greyb, E. N. Karlssonb, I. R. Meizosoa, and J. A. L. Pasténb, "Integrated process for sequential extraction of saponins, xylan and cellulose from quinoa stalks (Chenopodium quinoa Willd.)," Industrial Crops & Products, vol. 121, pp. 54-65, 2018.

[11] M. G. Saad, C. H. Chia, S. Zakaria, M. S. Sajap, S. Misran, M. H. Abdul Rahman, and S. Chin, "Physical and Chemical Properties of the Rice Straw Activated Carbon Produced from Carbonization and KOH Activation Processes," Sains Malaysiana, vol. 48, no. 2, pp. 385–391, 2019.

[12] S. Chen, S. Tang, Y. Sun, G. Wang, H. Chen, X. Yu, Y. Su, and G. Chen, "Preparation of a Highly Porous Carbon Material Based on Quinoa Husk and Its Application for Removal of Dyes by Adsorption,'' Materials, vol. 11, p. 1407, 2018.

[13] B. D. Gebrewold, P. Kijjanapanich, E. R. Rene, P. N. L. Lens, and A. P. Annachhatre, "Fluoride removal from groundwater using chemically modified rice husk and corn cob activated carbon," Environmental Technology, vol. 40, Issue 22, 2018.

[14] J. R. Hernandez, S. C. Capareda, and F. L. Aquino, "Activated Carbon Ptoduction From Pyrolysis And Steam Activation Of Cotton Gin Trach," Beltwide Cotton Conferences, New Orleans, Louisiana, vol. 9, no. 12, pp. 1494-1499, 2007.

[15] C.J. Piper, "Soil and plant analysis," inter". Sci. Puplishers inc.,New York, 1950.

[16] Y. Shinogi, H. Yoshida, T. Koizumi, M. Yamaoka, and T. Saito, " Basic characteristics of low-temperature carbon products from waste sludge," Adv. Environ. Res., vol. 7, pp. 661–665, 2003.

[17] AOAC, Official Methods of Analysis.17th Edition,The Association of Official Analytical Chemists, Gaithersburg, MD, USA, 2000.

[18] D. L. Rowel, "Soil Science. Methods and Applications," Longman Scientific and Technical, Harlow, Essex, UK, p. 350, 1994.

[19] G. A. Snedecor, and W. G. Cochran, "Statistical Methods," Iwoa State Univ. Press, Ames, 1994.

[20] F.A.S. Silva, and C.A.V. Azevedo, Principal Components Analysis in the Software Assistat-Statistical Attendance. In: World Congress on Computers in Agriculture, 7, Reno-NV-USA:American Society of Agricultural and Biological Engineers, PP. 393-396, 2009.

[21] L. Zhan, and M. Chen, "The Improvement Effects of Different Treatment Methods of Soil Wastewater Washing on Environmental Pollution," Water, vol. 12, p. 2329, 2020.

[22] D. Abril, V. Ferrer, Y. M. Gallardo, G. C. Barjas, C. Segura, A. Marican, A. Pereira, E. F. D. Lara, and O. Valdés, "Comparative Study of Three Dyes' Adsorption onto Activated Carbon from Chenopodium quinoa Willd and Quillaja saponaria," Materials, vol. 15, p. 4898, 2022.

[23] E. Wolak, and A. O. Zięba, "Change of the surface and structure of activated carbon as a result of HNO_3 modification," Springer, 2023.

[24] M. Gale, P. M. Nguyen, and K. L. G. AbdulAziz, "Synergistic and Antagonistic Effects of the Co-Pyrolysis of Plastics and Corn Stover to Produce Char and Activated Carbon," ACS Omega, vol. 8, pp. 380−390, 2023.

[25] J. H. Park, G. Choppala, S. J. Lee, N. Bolan, J. W. Chung, and M. Edrak, "Comparative Sorption of Pb and Cd by Biochars and Its Implication for Metal Immobilization in Soils," Water Air Soil Pollut, vol. 224, p. 1711, 2013.

[26] J. Komkiene, and E. Baltrenaite, "Biochar as adsorbent for removal of heavy metal ions

[Cadmium(II), Copper(II), Lead(II), Zinc(II)] from aqueous phase," Environ. Sci. Technol., vol. 13 , pp. 471–482, 2016.

[27] S. K. Shahcheragh, M. M. B. Mohagheghi, and A. Shirpay, "Efect of physical and chemical activation methods on the structure, optical absorbance, band gap and urbach energy of porous activated carbon," SN Applied Sciences, vol. 5, p. 313, 2023.

[28] M. Ullah, R. Nazir, M. Khan, W. Khan, M. Shah, S. G. Afridi, and A. Zada, "The effective removal of heavy metals from water by activated carbon adsorbents of Albizia lebbeck and Melia azedarach seed," Soil and Water Research, vol. 15, pp. 30–37, 2020.

[29] J. H. Lee, Y. J. Heo, and S.J. Park, "Effect of silica removal and steam activation on extra-porous activated carbons from rice husks for methane storage," international journal of hydrogen energy, vol. 43, pp. 22377-22384, 2018.

[30] Z. Peng, Y. Xu, W. Luo, C. Wang, and L. Ma," Conversion of Biomass Wastes into Activated Carbons by Chemical Activation for Hydrogen Storage, " ChemistrySelect, vol. 5, pp. 11221–11228, 2020.

[31] X. He, X. Chen, X. Wang, and L. Jiang, "Optimization of activated carbon production from corn cob using response surface methodology," Frontiers in Environmental Science, vol. 11, p. 5408, 2023.

[32] M. I. D. Helal, M. E. Husein, and W. G. E. D. Mostafa, "Characterization of Agricultural Residues- Based Nano Biochar and its efficiency in Adsorption/Desorption of Nutrients," International Journal of Environment, vol. 8, no. 2, pp. 130-141, ISSN: 2077-4508, 2019.

[33] H. A. El-Gawad, G. Kadry, H. A. Zahran, and M. H. Hussein, "Chromium Disarmament from Veritable Tanneries Sewer Water Utilizing Carbonic Rice Straw as a Sorbent: Optimization and Carbonic Rice Straw Characteristics," Water Air Soil Pollut, vol. 234, p. 659, 2023.

[34] J. Y. Lee, and B. J. Kim, "Surface-Modified Activated Carbon Fibers by a Facile Microwave Technique for Enhancing Hydrocarbon Adsorption," Environments, vol. , p. 52, 2023.

[35] C. T. Tovar, A. V. Ortíz, A. D. G. Delgado, A. H. Barros, Barros, and R .O. Toro, " Selective and Binary Adsorption of Anions onto Biochar and Modified Cellulose from Corn Stalks," Water, vol. 15, p.142, 2023.

[36] S. A. Borghei, M. H. Zare, M. Ahmadi, M. H. Sadeghi, A. Marjani, S. Shirazian, and M. Ghadiri, "Synthesis of multi-application activated carbon from oak seeds by KOH activation for methylene blue adsorption and electrochemical supercapacitor electrode," Arabian Journal of Chemistry, vol. 14, p. 102958, 2021.

[37] N. J. Hamadi, A. A. Mohammed, and A. H. Ali, "Removal of pb^{2+}, Cu^{2+} and Cd^{2+} Metals from Simulated Wastewater in Single and Competitive System Using Locally Porcelanite," International Journal of Engineering Sciences & Research Technology, vol. 3, no. 7, pp. 245-257, 2014.

[38] E. Menya, P. W. Olupot, H. Storz, M. Kiros, Y. Lubwama, and M. J. John, "Effect of alkaline pretreatment on the thermal behavior and chemical properties of rice husk varieties in relation to activated carbon production," Journal of Thermal Analysis and Calorimetry, vol. 139, pp. 1681–1691, 2020.

[39] T. T. H. Pham, "Investigation of activated carbon derived from rice straw biomass for removal of phenol from aqueous solution," Vietnam Journal of Science," Technology and Engineering, vol. 65, no. 1, pp. 43-46, 2023.

[40] L. B. Almalike, A. A. Al-Asadi, and A. S. Abdullah, "Adsorption of Lead and Cadmium Ions onto Soils: Isotherm Models, and Thermodynamic Studies," GU Journal of Science, vol. 33, no. 4, pp. 702-717, 2020.

[41] H. U. Rahim, W. A. Akbar, and J. M. Alatalo, "A Comprehensive Literature Review on Cadmium (Cd) Status in the Soil Environment and Its Immobilization by Biochar-Based Materials," Agronomy, vol. 12, pp. 877, 2022.

[42] S. Bashir, J. Zhu, Q. Fu, and H. Hu, "Comparing the adsorption mechanism of Cd by rice straw pristine and KOH-modified biochar," Environmental Science and Pollution Research, vol. 25, pp. 11875–11883, 2018.